

CE-STR-82-12

ASSESSMENT OF STRUCTURAL DAMAGE  
USING THE THEORY OF EVIDENCE

Sassan Toussi

James T. P. Yao

Supported by  
The National Science Foundation

through

Grant No. PFR 796296

March 1982

School of Civil Engineering  
Purdue University  
West Lafayette, IN 47907

Any opinions, findings, conclusions  
or recommendations expressed in this  
publication are those of the author(s)  
and do not necessarily reflect the views  
of the National Science Foundation.



ASSESSMENT OF STRUCTURAL DAMAGE  
USING THE THEORY OF EVIDENCE

by

Sassan Toussi  
and  
James T. P. Yao  
School of Civil Engineering  
Purdue University  
W. Lafayette, IN 47907

ABSTRACT

An attempt has been made to analyze dynamic test data of building structures for the assessment of structural damage. In this paper, the method of converting evidential information to the interval representation of Dempster and Shafer is applied. It is shown how results as obtained from an individual source are interpreted. Then, the information as obtained from several different sources is combined to compensate for individual deficiencies of the knowledge sources. The resulting algorithm is then applied to assess the damage state of a prototype 10-story reinforced concrete frame structure subjected to repeated earthquake loading conditions in the laboratory



## INTRODUCTION

Recently, several investigations have been conducted for the evaluation of structural damage by analysing recorded dynamic response of these structures [1-7]. A technique for the identification of inter-story hysteretic behavior of multi-story building structures was introduced by authors [4-6]. An interesting feature of these estimated load-deflection relationships is the "soft-to-stiff" type of behavior of reinforced concrete structures under large and repeatedly applied deflections. From this observation, Toussi [4] proposed a new damage indicator which is called "slope ratio" and defined as the ratio of structural stiffness under low-amplitude deflections (and loads) to that of the initial unloading at high-amplitude deflections (and loads). There exists uncertainty in the process of identification and computation, particularly in the treatment of highly nonlinear structures. Such an uncertainty results from the error/noise associated with measurement process and the mathematical representation of the system. This type of uncertainty, therefore, required further investigation of how the system identification results can be further refined.

Because there were alternative measures of damage as given by other investigators, it was decided to study techniques which can be used to combine the resulting

assessment of structural damage as obtained from several different sources. Because the range of variation in a subjective assessment cannot be expressed numerically, only inference procedures can be used to solve this problem in terms of words, phrases or statements. Consequently, new definitions and expressions are needed herein. Nevertheless, the emphasis of this paper is placed upon the engineering application of such a theory.

Garvey, Lowrance, and Fischler [8] introduced a method for the integration of knowledge accumulated from a variety of sources on the basis of the "evidential propositional calculus", which is a derivative of Shafer's mathematical theory of evidence [9]. This led authors to form a simple algorithm to combine the information as obtained from several different sources.

Dempster and Shafer's theory [9,10] can be used to provide a rational inference procedure for the solution of problems with uncertainty [11]. In contrast to the probabilistic techniques, which cannot be used to deal effectively with ignorance/uncertainty, Dempster and Shafer incorporated such an uncertainty into numerical computation. In their approach, it is not necessary to set the sum of the probability of a proposition (event) and its negation (complement) equal to one. The likelihood of a proposition,  $A$ , is presented as a subinterval  $[s(A), p(A)]$ , of the unit interval  $[0,1]$ . The evidential support for  $A$  is represented by  $s(A)$ , while  $p(A)$  represents the degree to

which one fails to doubt  $A$  and is equal to one minus the evidential support for  $\bar{A}$ . Because  $s(A)+s(\bar{A})\leq 1$ , it is inferred that  $s(A)\leq p(A)$ . The difference between the values of  $s(A)$  and  $p(A)$ , therefore, represents the degree of uncertainty of  $A$ .

In this paper, the method of converting evidential information, as furnished in the form of a probability mass distribution, to the interval representation is described. The basic principle of Dempster and Shafer's theory is first presented. Using an example, it is shown how to manipulate and interpret the results (samples) as obtained from an individual source in order to form a parameter mass distribution. The Dempster's rule of combination is then used to combine the information obtained from several different sources. This combination, as will be shown later, has the effect of compensating for the individual deficiencies of the knowledge sources. Finally, the proposed algorithm is used to assess the damage state of a prototype 10-story reinforced concrete frame structure subjected to simulated earthquake excitations.

## LITERATURE REVIEW

### Degree of Support and Doubt

The Shafer's representation is used herein to indicate the degree of support and doubt of a proposition. The likelihood of proposition  $A$  is expressed with a subinterval,  $[s(A), p(A)]$ , of the unit interval,  $[0,1]$ . The lower value,  $s(A)$ , represents the "support" for the proposition, while the upper value,  $p(A)$ , indicates the degree to which one fails to doubt  $A$ . "Support" may be interpreted as the total positive effect a body of evidence has on a proposition, while  $p(A)$  represents the total extent to which a body of evidence fails to refute a proposition [8]. The degree of uncertainty of  $A$  is the difference between the upper and the lower probability values (i.e.  $p(A)-s(A)$ ).

For instance, if there is no information about  $A$ , the Shafer's representation becomes  $A_{[0,1]}$ ; while  $A_{[1,1]}$  and  $A_{[0,0]}$  indicate that  $A$  is true or false, respectively. A partial support for  $A$  might be indicated by  $A_{[0.30,0.85]}$  while  $A_{[0.30,1]}$  expresses a firm support for  $A$ . Finally, a partial support for  $\bar{A}$  can be shown by  $A_{[0,0.3]}$ .

### Frame of Discernment

The frame of discernment,  $\Theta$ , is a set whose subsets are propositions. When a proposition corresponds to a subset of a frame of discernment, it means that the frame discerns that proposition. This is most effective when one is



concerned with the true value of a quantity. If the quantity is indicated by  $\theta$  and the set of its possible values by  $\Theta$ , then the propositions of interest are precisely those of the form "the true value of  $\theta$  is in  $T$ ", where  $T$  is a subset of  $\Theta$ . It should be noted that the "possibilities" that comprise  $\Theta$  will get meaning from what we know or think we know and it is not independent of our knowledge [9].

The primary advantage of this formation is that it translates the logical notions of conjunction, disjunction, implication, and negation into the set-theoretic notions of intersection, union, inclusion, and complementation.

#### Simple Belief Function

It is assumed that a knowledge source,  $KS_j$ , provides evidential information about a set of propositions. This information can be presented by a function, belief function, as follows:

$$m_j : \{A_i \mid A_i \subset \Theta\} \rightarrow [0,1]$$

$$m_j(\phi) = 0.0$$

$$\sum_i m_j(A_i) = 1$$

where  $A_i$  are subsets of  $\Theta$  (i.e.  $A_i \subset \Theta$ ). The "basic probability mass",  $m_j(A_i)$ , represents a measure of the belief that  $KS_j$  has committed exactly to proposition  $A_i$ . Therefore,  $m_j$  may be visualized as a partitioned unit line segment, and the length of each subsegment corresponds to the mass contributed to that subsegment by  $KS_j$  as shown in Figure 1-a. The mass assigned to  $\Theta$  is assumed to be distributed in some unknown manner among the propositions

discerned by  $\theta$ . In fact,  $m_j(\theta)$  represents the residual "uncertainty" of the  $KS_j$  directly. Once the masses assigned to the propositions are obtained, the evidential intervals,  $[s(A_i), p(A_i)]$  can be determined directly.

The Total support for proposition  $A_i$  is given by the sum of the masses assigned to  $A_i$  and to the subsets of  $A_i$ :

$$S_j(A_i) = \sum_k m_j(D_k)$$

where  $D_k \subset A_i$ . The plausibility of  $A_i$ ,  $P(A_i)$ , is, on the other hand, one minus the sum of the masses assigned to  $\bar{A}_i$  and to the subsets of  $\bar{A}_i$ :

$$P_j(A_i) = 1 - \sum_k m_j(B_k)$$

where  $B_k \subset \bar{A}_i$ . Consequently the uncertainty of  $A_i$  is obtained by:

$$U_j(A_i) = P_j(A_i) - S_j(A_i)$$

#### Dempster's Rule of Combination

Dempster [10] introduced a technique to combine the information as supplied by different knowledge sources. A belief function which is constructed to represent an evidence can be combined with another belief function, representing another evidence, in order to pool the information obtained from these two knowledge sources. Dempster's rule deals symmetrically with the two knowledge sources and does not depend upon the priority of either one of them. The combination of two belief functions is called "orthogonal sum", and it is illustrated with the unit square as shown in Figure 1. This figure shows how the two line segments representing  $m_1$  and  $m_2$  are orthogonally combined

and formed a unit square. In this square, for example, a vertical strip of measure  $m_1(A_i)$  that is exactly committed to  $A_i$  by  $KS_1$  (Knowledge source 1) and a horizontal strip of measure  $m_2(B_j)$  that is exactly committed to  $B_j$  by  $KS_2$  are shown. The intersection of these strips forms a square of  $m_1(A_i)m_2(B_j)$  area which is indeed a measure of belief in  $A_i \cap B_j$ . Sometimes, a given subset of  $\Theta$ ,  $C$ , may have more than one rectangle exactly committed to it, thus the total mass allocated to  $C$  is:

$$m(C) = \sum m_1(A_i)m_2(B_j)$$

Where  $A_i \cap B_j = C$ . There is the possibility of committing a portion of mass to the empty set  $\phi$ . In fact every rectangle committed to  $A_i \cap B_j$ , where  $A_i \cap B_j = \phi$ , results in such a commitment. The remedy is to discard all such rectangles and proportionally increase the size of the remaining rectangles by the following factor:

$$N = [1 - \sum m_1(A_i)m_2(B_j)]^{-1}$$

where  $A_i \cap B_j = \phi$ . Therefore, the total probability mass will again have measure one.

The degree of conflict between two knowledge sources depends on the inverse value of factor  $N$ . The smaller the inverse value of  $N$ , the greater the degree of conflict between the knowledge sources. It is clear when the inverse value becomes zero, the orthogonal sum can not exist.

#### Combining Several Belief Functions

Simply by repeating the rule of combination, any number of belief functions can be combined. The process is as

follows:

$$\text{Bel}_1 + \text{Bel}_2$$

$$(\text{Bel}_1 + \text{Bel}_2) + \text{Bel}_3$$

$$((\text{Bel}_1 + \text{Bel}_2) + \text{Bel}_3) + \text{Bel}_4$$

etc.

It is continued until all the  $\text{Bel}_i$  are included. From the equations, once again, it is recognized that the Dempster's rule of combination is independent of the priority of the knowledge sources ( $\text{KS}_j$ ).

## APPLICATION

In the preceding sections, the necessary rules and the basic assumptions of Dempster and Shafer's theory were summarized. It is desirable to apply this theory to solve practical engineering problems. Because the present application is to determine the damage state of an existing structure, the frame of discernment is the set of possible states of damage. It is assumed herein that there are four possible states of damage { S, L, D, C }, where S, L, D, and C denote "Safe", "Lightly damaged", "Damaged", and "Critically damaged", respectively. Two features, namely "slope ratio" and "drift ratio", are considered as the damage state parameters. The information about the parameter values is presented in the form of parameter mass distribution graphs such as those shown in Figure 3. These curves indicate the probability of any state of damage for a given parameter value. To develop a damage parameter mass distribution, information regarding the damage state of a prototype structural frame, which had gone under a series of successive dynamic tests is used. Then the information about the states of damage of another dynamically tested structure, is used to evaluate the developed parameter mass distributions. It should be noted, in the foregoing sections, that the terminologies "training samples" and "testing samples" refer to the information used to develop

and to test the parameter mass distributions, respectively.

#### Training Samples (Test structure H2)

Cecen [12], using the shaking table of the University of Illinois, recorded the response of a one-tenth scale and ten-story structural frame subjected to a series of simulated earthquakes. The simulated earthquakes were patterned after the north-south component of the acceleration history as recorded in El-Centro during the Imperial Valley earthquake of 1940. The test structure was subjected to seven successive earthquake test runs. The base motion intensities were incrementally increased with each successive run.

Toussi and Yao [5,6] used the measured acceleration response histories to identify the inter-story hysteretic behavior of the test structure. Figure 2 shows the estimated hysteretic behavior of the seventh floor of the test structure during seven different test runs. The existence of a "soft-to-stiff" property in the structure's behavior becomes more apparent as the structure experiences larger deflections.

Table 2, under the columns labeled "slope", represents the slope ratios calculated for each floor at different test runs. The drift ratio is used as another measure of damage [3]. Although there does not exist any effective device for measuring the lateral displacement of existing high-rise buildings, Toussi [4] has shown that it is possible to obtain the displacement histories from the recorded

acceleration responses. Using a proper filtering technique to filter out the noise in the acceleration response and then integrating twice the filtered acceleration response yield the displacement response time-history. Table 2, under the columns labeled "drift", also indicates the drift ratios .

The classification of the damage state of a floor of the test structure H2 results from three different pieces of information: comments and reports made by Cecen [12] who tested and analysed the measured response of H2, the crack patterns , and the hysteretic behavior of floors identified by Toussi and Yao [4,5].

#### Recorded Response Histories

An interesting feature of the response histories is their flat, nonperiodical portions around the time  $t=2$  seconds. These irregularities become more apparent after the second run of the test structure. The fact that a similar irregularity is observed in the input motion indicates that this is an inherent characteristic of the prototype base motion. The reflection of the irregularities in the structure's response doesn't appear until the structure becomes sufficiently softened. The general softening of the structure becomes more apparent as the higher-mode vibrations take a more dominant role on the acceleration response histories for the later tests.

Cecen [12] indicated that the variation of the top-level displacement and acceleration response with the

spectrum intensity of the base motion had a clearly defined linear form. Only the maximum top-level displacement, measured at the last run, deviated from the linear variation. This observation may be inferred as a significant change in the behavior of the H2 frame during the last run.

Since the variation of the maximum base and overturning moment with top-level displacement (double amplitude/2) had the same trends (with a yield point corresponding to a maximum top displacement of 16mm), it was concluded that the structure was within the linear response range during its first two runs.

From these observations and the reported changes in the dynamic properties of the H2 frame [12], the following conclusions regarding the floor damage states are made. The structure was safe after the first and the second test runs. At the end of the third and fourth, the structure was lightly damaged. While it was damaged during the fifth test run, at the end of the sixth and seventh, the structure was visibly unsafe.

#### Crack Patterns

From crack patterns and other observations by Cecen and his colleagues, a brief description of crack development is followed. During the first run, only shrinkage and other minor cracks were developed and no major new cracks were observed. The structure experienced new cracks during the second run and some of the shrinkage cracks opened up more



(all the crack widths remained within 0.05mm). New cracks developed during the third run and crack widths exceeded 0.1mm (some flexural cracks were observed especially on the base columns). The crack pattern practically remained the same at the end of the fourth test run.

During the fifth test run, the structure experienced few flexural cracks, which were mostly on the beam ends of the fourth through eighth floors, and crack widths increased to 0.3mm. The sixth run created more cracks mainly on the beam ends of the third, fourth, and ninth floors. In addition, a few cracks appeared on the tenth story and crack widths were around 0.4mm. Finally, some spalling and crushing of concrete, at beam ends of the sixth and seventh floors, were observed at the end of the seventh run.

Although there is no limit specifying the severity of cracks, cracks within a range of 0.3 to 0.5mm are considered as severe cracks and spalling and crushing of concrete are the indication of the severest situation. Finally, cracks within a range of 0.1 to 0.3mm are considered as moderate cracks. Therefore, according to the above specified ranges and the location of the concentrated cracks, the damage state of floors are concluded and listed in Table 1 under the columns labeled "C".

#### Hysteretic Behaviors

Figure 2 represents the inter-story hysteretic behavior of the seventh floor identified by using authors' system identification technique[4-6]. Although there are

restrictions on the applications of their technique [4], the technique is successful in the detection of the progress from linear, to slightly non-linear, and finally to highly non-linear behavior of the structure. Behaviors such as the one shown in Figure 2-f may not be the indication of a critical situation, it is reasonable to be used as an indication of relatively damaged states.

The damage states of floors are classified accordingly: a linear, semi-linear, bi-linear, and unrecognizable load-deflection behavior are respectively referring to a safe, lightly damaged, damaged, and critically damaged structure.

#### Formation of Damage Parameter Mass distributions

Table 1 represents the classes assigned to different values of the slope and drift ratios. The classification was concluded from the information as furnished by three different sources. A graphical representation of their mass distributions with the levels of damage is presented in Figure 3. Since there does not exist sufficient number of samples, a statistical calculation can not be made for the determination of the form of the parameter mass distributions. A triangular mass distribution is selected for its simplicity, and the area under each curve is normalized to to be unity. These curves possess the two properties as follows. First, they show the range of variation of the propositions with the parameter values. Second, for a given value of a parameter, each mass distribution assigns a number; the number presents how much

the parameter (specified with its numerical value) is believed to belong to that proposition.

#### Testing Samples (Test Structure MF1)

The MF1 test structure was a one-tenth scale, ten-story reinforced concrete frame which was dynamically tested at the University of Illinois [13]. The dynamic test procedure included a series of strong base motions, simulating a selected version of the north-south component of the El-Centro earthquake of 1940. Healy and Sozen [13] described their experimental work and presented the acceleration and displacement data recorded in three earthquake simulation tests.

Toussi and Yao [4-6] applied their system identification technique to the acceleration response histories and estimated the inter-story hysteretic behaviors of floors as shown in Figure 4. The slope ratios [4] are listed under the columns labeled "slope" in Table 3. The drift ratios [13] are listed in the same table but under the columns labeled "drift". These information are used to determine the most likely damage states of various stories in the test structure.

From the developed damage parameter mass distributions, a set of numbers is obtained for a given parameter value. Then, by normalizing the resultant numbers to bring their total sum equal to one, a set of "basic mass numbers" is computed. As mentioned earlier, there exists uncertainty with any given knowledge source. The uncertainty  $U$  of the

knowledge source is considered through reducing each basic mass numbers by a multiplication factor which is equal to one minus  $U$ . This new set of mass numbers is used to represent the contribution of the knowledge source to the support of the proposition. Since there are two sets of mass numbers for each floor (one obtained for the measured slope ratio and the other for the measured drift ratio), Dempster's rule of combination is used to combine these two sets. The results of this combination are used to get an understanding of the degree of damage which occurred to each floor during any one of the three successive test runs.

To evaluate the proposed algorithm, a similar procedure which was used for the classification of H2-frame floors' damage states is also conducted for the MF1 structure. Then a comparison between the results of this classification and those of the proposed algorithm is made to find how effective and accurate the algorithm is.

#### Computation

The computation starts with the conversion of the measured parameters (damage and drift ratios) into a set of probability numbers which specify the contribution of each proposition (i.e. S, L, D, and C) in the damage occurred to structure. Table 3 contains the measured slope and drift ratios of floors. Each parameter mass distribution yields a set of numbers which by normalizing the numbers to bring their sum to one, a set of "basic mass numbers" is obtained for each floor. This process is, in

fact, the computation of the probability of each proposition, which is conditioned upon the measured parameter's falling in the specified range. Assuming an uncertainty of 0.3 for SR measurement and an uncertainty of 0.2 for DR measurement, the resulting mass functions are shown in Tables 4 and 5, respectively. Combining the corresponding mass functions with Dempster's rule of combination yields the composite mass functions (Table 6). In this table, the columns labeled "0" represents the uncertainty in the corresponding belief functions. To show how the above procedure was conducted, the measured parameters of an arbitrarily-chosen floor are taken and the calculation is followed step by step.

#### Example

The knowledge sources have reported a slope ratio of 0.284 and a drift ratio of 0.035 for the first floor after the second test run. The S, L, D, and C triangles as shown in Figure 3 yield respectively 0.0, 4.6, 1.0, and 0.0 for the estimated slope ratios; and 0.0, 0.0, 17.0 and 0.0 for the estimated drift ratios.

Assuming an uncertainty of 0.3 in the SR measurement and an uncertainty of 0.2 in the DR measurement, and normalizing the obtained initial mass functions yield the following mass functions:

$$m_{sr}(\langle S, L, D, C \rangle) = \langle 0.0, 0.57, 0.13, 0.0 \rangle$$

and

$$m_{dr}(\langle S, L, D, C \rangle) = \langle 0.0, 0.0, 0.40, 0.4 \rangle$$

Combining  $m_{sr}$  and  $m_{dr}$  with Dempster's rule gives the composite mass function:

$$m_{sr \ dr}(\langle S, L, D, C \rangle) = \langle 0.00, 0.22, 0.41, 0.24 \rangle$$

with a resulting uncertainty of 0.12. This combination is illustrated in Figure 5 in which all rectangles attributed to  $\phi$  are shaded and the remaining rectangles labeled with the proposition receiving that mass. These values are converted directly to the following intervals on the propositions:  $S[0.00, 0.12]$ ,  $L[0.22, 0.34]$ ,  $D[0.41, 0.53]$ ,  $C[0.24, 0.36]$ . From these intervals, it is inferred that the first floor has sustained a moderate level of structural damage.

## CONCLUSION

Results as listed in Table 8 indicate that five out of twenty five cases of damage assessments made by using the proposed algorithm are likely to be incorrect. A twenty percentage error is acceptable considering the fact that the lack of sufficient samples did not permit an effective statistical analysis for the determination of the damage parameter mass distribution to be made. Moreover, only two features are used herein. In practice, there are usually other features available for damage assessment of existing structures.

The most significant feature of the algorithm is the consideration of the different pieces of information in a simultaneous fashion. No priority is given to any source of knowledge and, consequently, not any iteration procedure is needed for updating process.

## ACKNOWLEDGEMENT

This investigation is supported in part by the National Science Foundation under Grant No. PFR-796296. The authors would like to express their appreciation to Dr. M. Ishizuka for his constructive suggestions. They are also thankful to Professors M. A. Sozen, R. H. Lee and C. D. Sutton for their helpful comments.



## REFERENCES

- [1] Chen, S.J.H. and Yao, J.T.P., "Identification of Structural Damage Using Earthquake Response Data," Proceedings at the ASCE EMD-STD Specialty Conference, Austin, Texas, September 17-19, 1979, pp. 661-664.
- [2] Galambos, T.V., and Mayes, R.I., Dyanmic Test of a R/C Building, Dept. of Civil Engineering and Applied Science, Washington University, St. Louis, Missouri, June 1978.
- [3] Sozen, M.A., Review of Earthquake of R/C Buildings with a View to Drift Control, Presented at 7WCEE, Turkey, September 1980.
- [4] Toussi, S., System Identification Methods for the Evaluation of Structural Damage, Ph.D. Thesis, (in preparation).
- [5] Toussi, S., and Yao, J.T.P., Identification of Hysteretic Behavior for Existing Structures, Technical Report No. CE-STR-80-19, School of Civil Engineering, Purdue University, W. Lafayette, IN, December 1980.
- [6] Toussi, S. and Yao, J.T.P., Hysteresis Identification of Multi-Story Building, Technical Report No. CE-STR-81-15, School of Civil Engineering, Purdue University, W. Lafayette, IN, May 1981.
- [7] Yao, J.T.P., Toussi, S., and Sozen, M.A., Damage Assessment from Dynamic Response Measurements, Invited Paper, to be presented in the Symposium on Structural Reliability and Damage Assessment, Ninth U.S. National Conferece on Applied Mechanics, Cornell University, Ithaca, N.Y., 21-25, June 1982.
- [8] Garvey, T.D., Lowrance, J.D., and Fischler, M.A., "An Inference Technique for Integrating Knowledge from Disparate Sources," Proceedings of the Seventh International Joint Conference on Artificial Intelligence, Vancouver, British Columbia, Canada, August 1981.
- [9] Shafer, G., A Mathematical Theory of Evidence, Princeton University Press, 1976.
- [10] Dempster, A.P., "Upper and Lower Probabilities Induced by a Multi-Valued Mapping," Annals of Mathematical Statistics, Vol. 38, pp. 325-339, 1967.
- [11] Ishizuka, M., Fu, K.S., and Yao, J.T.P., Inference Procedure with Uncertainty for Problem Reduction Method, Technical Report CE-STR-81-24, School of Civil Engineering, Purdue University, August 1981.
- [12] Cecen, H., Response of Ten-Story Reinforced Concrete Frames to Simulated Earthquakes, Ph.D. Thesis, School of Civil Engineering, University of Illinois, Urbana, Illinois, March 1979.
- [13] Healy, T.J. and Sozen, M.T., Experimental Study of The Dynamic Response of a Ten-Story Reinforced Concrete Frame with a Tall First Story, Civil Engineering Studies, Structural Research Series No. 450, University of Illinois, August 1978.

	1st Run				2nd Run				3rd Run				4th Run				5th Run				6th Run				7th Run							
	R	Cr	I	F	R	Cr	I	F	R	Cr	I	F	R	Cr	I	F	R	Cr	I	F	R	Cr	I	F	R	Cr	I	F	R	Cr	I	F
1st Floor	S	S	S	S	S	L	S	S	L	D	L	L	L	D	L	L	D	D	L	D	C	D	C	C	C	C	*	C				
2nd Floor	S	S	S	S	S	L	S	S	L	D	L	L	L	D	L	L	D	D	L	D	C	D	C	C	C	C	*	C				
3rd Floor	S	S	S	S	S	L	L	L	L	L	L	L	L	L	L	L	D	D	L	D	C	C	D	C	C	C	*	C				
4th Floor	S	S	S	S	S	L	L	L	L	L	L	L	L	L	L	L	D	C	D	D	C	C	C	C	C	C	C	C				
5th Floor	S	S	S	S	S	L	D	L	L	L	L	L	L	L	L	L	D	C	D	D	C	D	D	D	C	C	C	C				
6th Floor	S	S	S	S	S	L	D	L	L	L	L	L	L	L	L	L	D	C	D	D	C	D	D	D	C	C	C	C				
7th Floor	S	S	S	S	S	L	L	L	L	L	L	L	L	L	L	L	D	C	D	D	C	D	D	D	C	C	C	C				
8th Floor	S	S	S	S	S	L	L	L	L	L	L	L	L	L	L	L	D	C	C	C	C	D	D	D	C	C	C	C				
9th Floor	S	S	S	S	S	L	S	S	L	L	L	L	L	L	L	L	D	D	C	D	C	C	C	C	C	C	C	C				
10th Floor	S	S	S	S	S	L	S	S	L	L	L	L	L	L	L	L	D	D	C	D	C	D	C	C	C	C	C	C				

TABLE 1: Damage state Classification of H2-Frame Floors for Seven Test Runs

Note: "R" - response histories, "Cr" - crack patterns, "I" - hysteretic behavior, "F" - final decision from R, C, and I (majority rule) "\*" - no response available.

	1st Run			2nd Run			3rd Run			4th Run			5th Run			6th Run			7th Run		
	Slope	Drift	Class	Slope	Drift	Class	Slope	Drift	Class	Slope	Drift	Class	Slope	Drift	Class	Slope	Drift	Class	Slope	Drift	Class
1st Floor	1.0	0.0	S	0.286	0.0	S	0.30	0.004	L	0.230	0.004	L	0.083	0.009	D	?	0.013	C	*	0.035	C
2nd Floor	1.0	0.0	S	0.412	0.004	S	0.25	0.009	L	0.215	0.009	L	0.250	0.017	D	?	0.026	C	*	0.052	C
3rd Floor	1.0	0.004	S	0.375	0.004	L	0.375	0.009	L	0.450	0.009	L	0.160	0.017	D	0.205	0.026	C	*	0.057	C
4th Floor	1.0	0.004	S	0.364	0.009	L	0.224	0.013	L	?	0.013	L	?	0.022	D	?	0.031	D	0.0	0.039	C
5th Floor	0.370	0.004	S	0.333	0.009	L	0.350	0.012	L	0.200	0.017	L	0.174	0.022	D	0.146	0.039	D	?	0.048	C
6th Floor	1.0	0.004	S	?	0.009	L	0.250	0.009	L	0.198	0.009	L	0.274	0.017	D	0.118	0.031	D	?	0.039	C
7th Floor	1.0	0.005	S	0.286	0.013	L	0.210	0.013	L	0.200	0.013	L	0.214	0.017	D	0.0	0.022	D	0.0	0.035	C
8th Floor	1.0	0.004	S	0.210	0.009	L	0.200	0.013	L	?	0.013	L	?	0.017	C	0.24	0.022	D	0.0	0.031	C
9th Floor	1.0	0.005	S	0.417	0.008	S	?	0.011	L	?	0.011	L	?	0.013	D	0.0	0.017	C	0.0	0.026	C
10th Floor	1.0	0.003	S	0.333	0.005	S	0.173	0.006	L	?	0.006	L	?	0.009	D	0.0	0.013	C	0.0	0.17	C

TABLE 2: Slope and Drift ratios of Test Structure H2

	1st Run		2nd Run		3rd Run	
	Slope	Drift	Slope	Drift	Slope	Drift
1st Floor	1.00	.017	0.284	0.035	0.065	0.043
2nd Floor	1.00	.015	0.304	0.030	0.144	0.036
3rd Floor	1.00	0.017	0.308	0.039	0.136	0.043
4th Floor	1.00	0.009	0.273	0.023	0.161	0.036
5th Floor	1.00	0.010	0.50	0.009	0.205	0.007
6th Floor	1.00	0.008	0.57	0.033	0.125	0.053
7th Floor	1.00	0.009	0.406	0.017	?	0.023
8th Floor	1.00	0.003	0.579	0.008	?	0.015
9th Floor	1.00	0.006	0.27	0.010	?	0.024
10th Floor	1.00	0.003	?	0.009	?	0.006

TABLE 3: Slope and Drift ratios of Test Structure MFl.

	1st Run				2nd Run				3rd Run			
	S	L	D	C	S	L	D	C	S	L	D	C
1st Floor	.70	0.0	0.0	0.0	0.0	0.57	0.13	0.0	0.0	0.0	0.17	0.53
2nd Floor	.70	0.0	0.0	0.0	0.0	0.7	0.0	0.0	0.0	0.11	0.42	0.17
3rd Floor	.70	0.0	0.0	0.0	0.02	0.68	0.0	0.0	0.0	0.09	0.37	0.24
4th Floor	.70	0.0	0.0	0.0	0.0	0.47	0.23	0.0	0.0	0.12	0.43	0.15
5th Floor	.70	0.0	0.0	0.0	0.70	0.0	0.0	0.0	0.0	0.22	0.48	0.0
6th Floor	.70	0.0	0.0	0.0	0.70	0.0	0.0	0.0	0.0	0.06	0.33	0.31
7th Floor	.70	0.0	0.0	0.0	0.16	0.54	0.0	0.0	0.0			
8th Floor	.70	0.0	0.0	0.0	0.7	0.0	0.0	0.0	0.0			
9th Floor	.70	0.0	0.0	0.0	0.0	0.47	0.23	0.0	0			
10th Floor	.70	0.0	0.0	0.0								

TABLE 4: Mass Functions calculated for Floors' Slope Ratios.

	1st Run				2nd Run				3rd Run			
	S	L	D	C	S	L	D	C	S	L	D	C
1st Floor	0.0	0.44	0.27	0.09	0.0	0.0	0.4	0.4	0.0	0.0	0.25	0.55
2nd Floor	0.0	0.49	0.24	0.07	0.0	0.0	0.45	0.35	0.0	0.0	0.40	0.40
3rd Floor	0.0	0.44	0.27	0.09	0.0	0.0	0.39	0.41	0.0	0.0	0.25	0.55
4th Floor	0.06	0.48	0.20	0.06	0.0	0.30	0.35	0.15	0.0	0.0	0.40	0.40
5th Floor	0.07	0.49	0.20	0.04	0.06	0.48	0.20	0.06	0.31	0.31	0.14	0.04
6th Floor	0.06	0.47	0.18	0.09	0.0	0.0	0.44	0.36	0.0	0.0	0.0	0.8
7th Floor	0.06	0.48	0.20	0.06	0.0	0.44	0.27	0.09	0.0	0.30	0.35	0.15
8th Floor	0.67	0.09	0.04	0.0	0.07	0.47	0.18	0.09	0.0	0.49	0.24	0.07
9th Floor	0.46	0.23	0.09	0.02	0.07	0.49	0.20	0.04	0.0	0.28	0.36	0.16
10th Floor	0.67	0.09	0.04	0.0	0.06	0.48	0.20	0.06	0.46	0.23	0.09	0.02

TABLE 5: Mass Functions calculated for Floors' Drift Ratios.

	1st Run					2nd Run					3rd Run				
	S	L	D	C	θ	S	L	D	C	θ	S	L	D	C	θ
1st Floor	0.26	0.26	0.11	0.06	0.11	0.0	0.22	0.41	0.24	0.12	0.0	0.0	0.19	0.73	0.08
2nd Floor	0.32	0.34	0.16	0.05	0.14	0.0	0.30	0.33	0.23	0.14	0.0	0.03	0.55	0.33	0.09
3rd Floor	0.26	0.26	0.11	0.06	0.11	0.00	0.33	0.26	0.27	0.14	0.0	0.03	0.35	0.53	0.09
4th Floor	0.42	0.28	0.12	0.04	0.12	0.0	0.48	0.36	0.07	0.09	0.0	0.04	0.56	0.31	0.09
5th Floor	0.41	0.31	0.14	0.02	0.12	0.41	0.29	0.13	0.04	0.13	0.16	0.35	0.37	0.02	0.11
6th Floor	0.34	0.23	0.08	0.05	0.10	0.32	0.0	0.30	0.25	0.14	0.0	0.02	0.10	0.79	0.09
7th Floor	0.42	0.28	0.12	0.04	0.12	0.04	0.71	0.12	0.04	0.09					
8th Floor	0.90	0.03	0.01	0.00	0.07	0.42	0.29	0.10	0.06	0.13					
9th Floor	0.78	0.08	0.04	0.01	0.09	0.03	0.65	0.22	0.01	0.08					
10th Floor	0.90	0.03	0.01	0.00	0.07										

TABLE 6: Composition of the Mass Functions of H2.

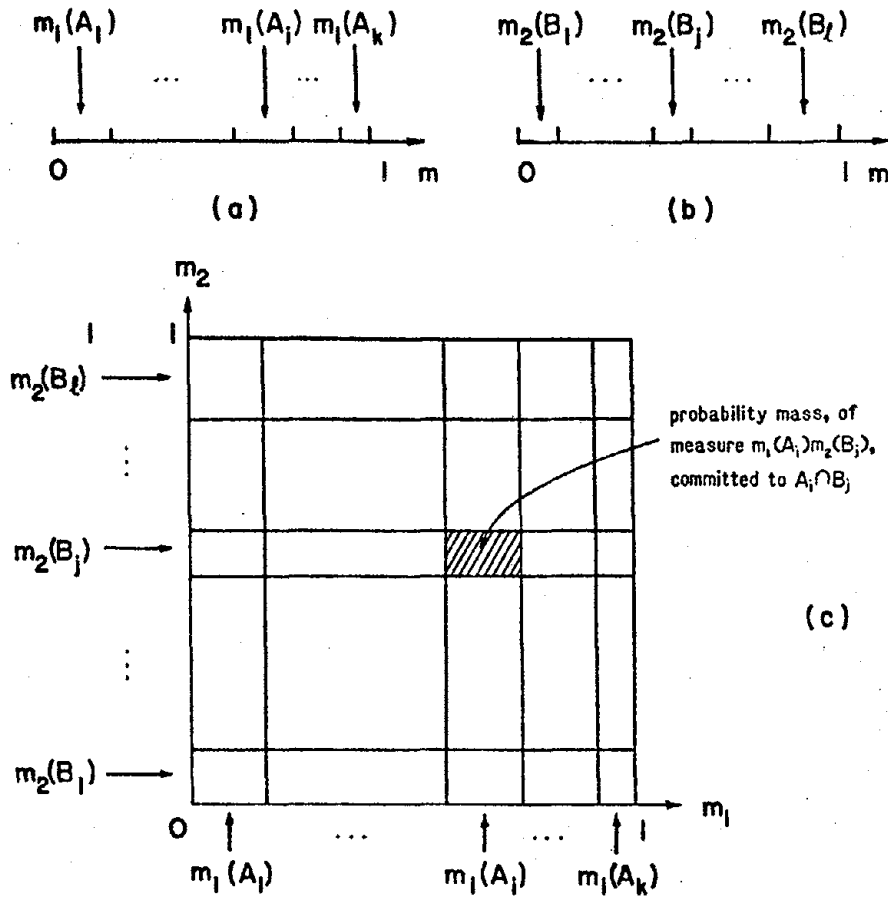
	1st Run				2nd Run				3rd Run			
	R	Cr	I	F	R	Cr	I	F	R	Cr	I	F
1st Floor	L	L	S	L	L	D	D	D	C	C	D	C
2nd Floor	L	L	S	L	D	D	D	D	C	C	D	C
3rd Floor	L	S	S	S	D	L	L	L	C	C	D	C
4th Floor	L	S	S	S	D	L	L	L	D	C	D	D
5th Floor	L	S	S	S	L	L	L	L	D	C	D	D
6th Floor	L	S	S	S	D	L	L	L	C	C	D	C
7th Floor	L	S	S	S	D	L	L	L	D	C	C	C
8th Floor	L	S	S	S	L	L	L	L	D	C	C	C
9th Floor	L	S	S	S	L	L	L	L	D	C	C	C
10th Floor	L	S	S	S	L	L	D	L	D	C	C	C

TABLE 7: Damage State Classification of MF1.



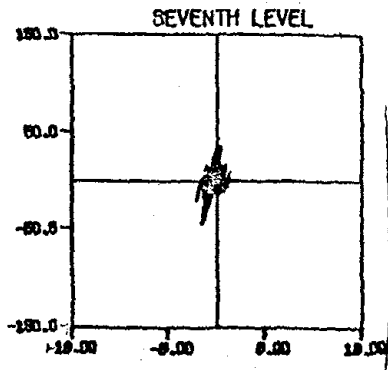
1st Run		2nd Run		3rd Run	
Algori- thm	Classi- fication	Algori- thm	Classi- fication	Algori- thm	Classi- fication
S	L	D	D	C	C
L	L	D	D	D	C
S	S	L	L	C	C
S	S	L	L	D	D
S	S	S	L	D	D
S	S	D	L	C	C
S	S	L	L		C
S	S	S	L		C
S	S	L	L		C
S	S				C

TABLE 8: Comparison Between Results  
Obtained by the Algorithm  
and the Classification.

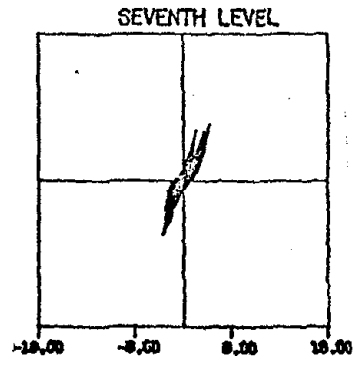


**FIGURE 1**

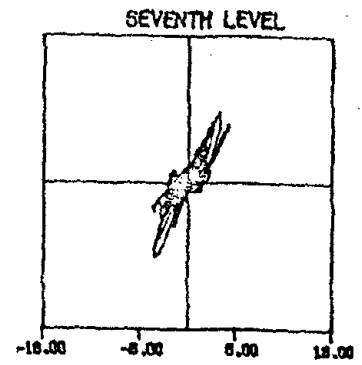
**Dempster's Rule of Combination**



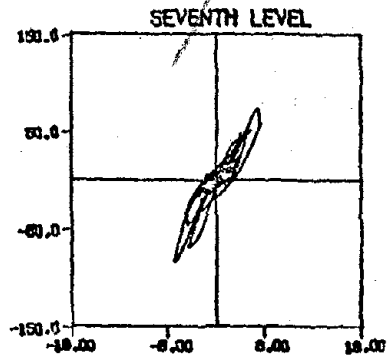
(a) Run 1



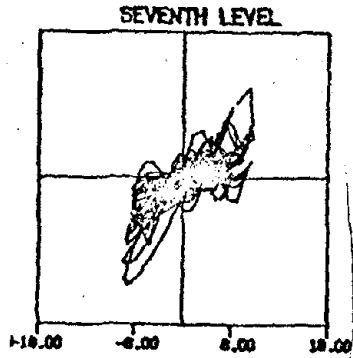
(b) Run 2



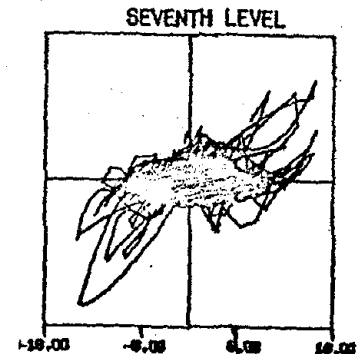
(c) Run 3



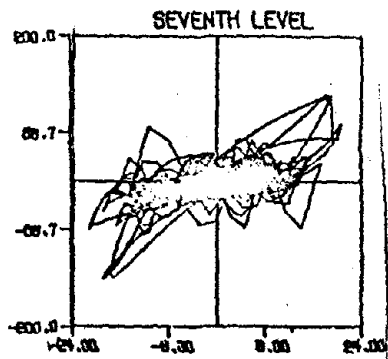
(d) Run 4



(e) Run 5



(f) Run 6



(g) Run 7

Figure 2: Identified Hysteretic Behavior of H2 Floors.

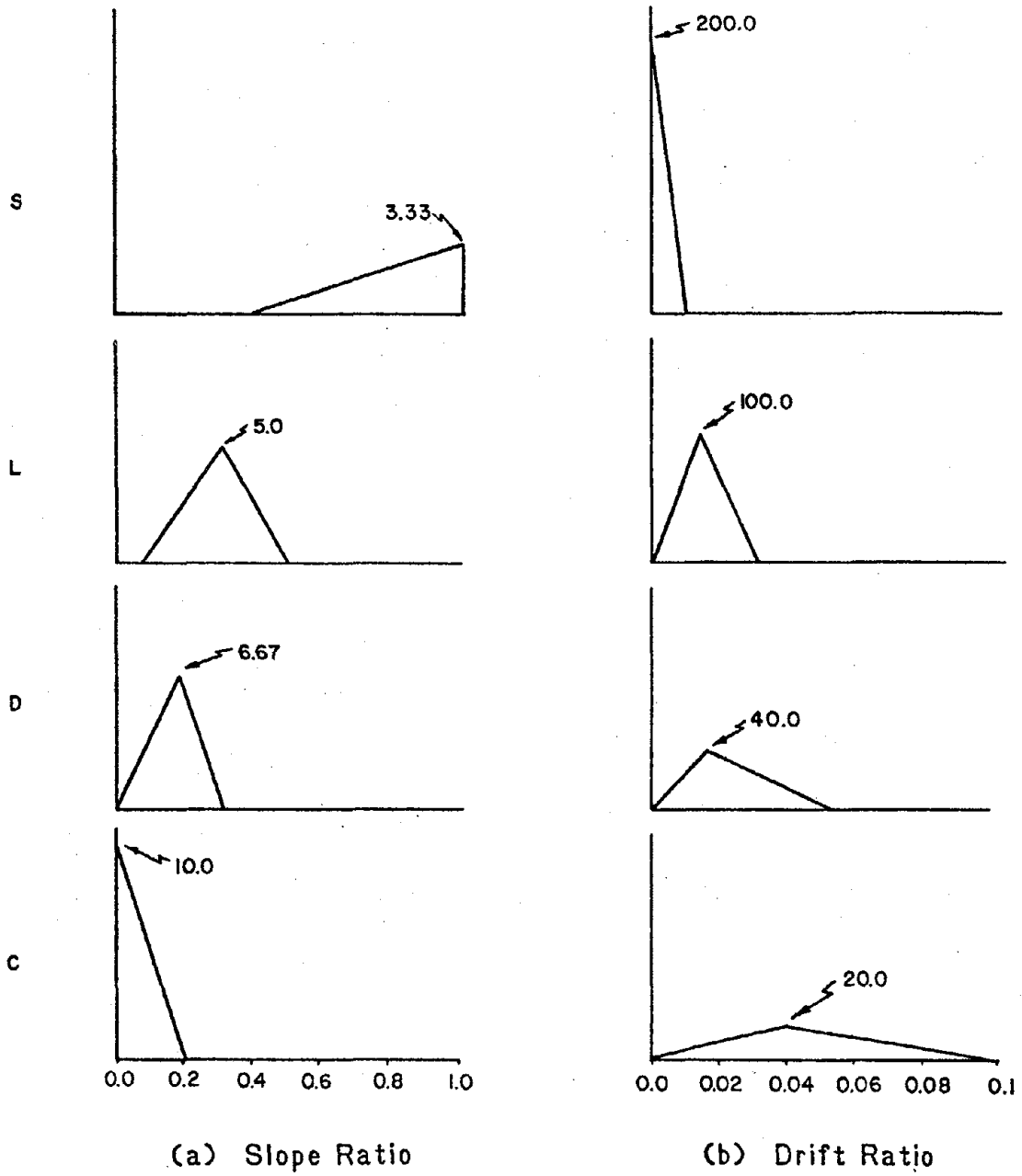
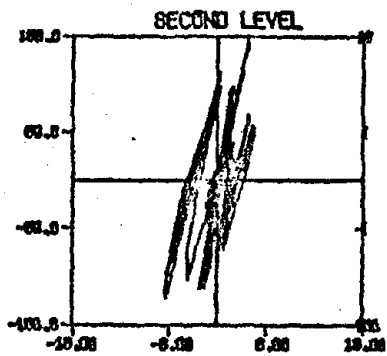
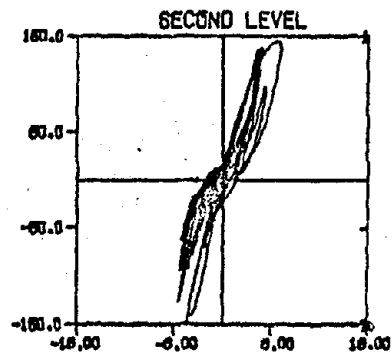


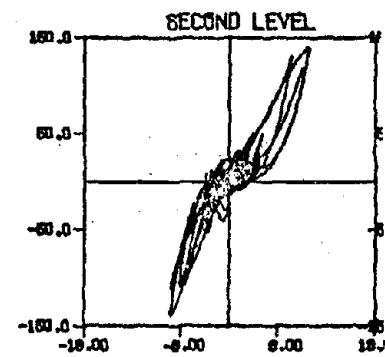
**FIGURE 3: Damage Parameter Distributions**



(a) Run 1



(b) Run 2



(c) Run 3

Figure 4: Identified Hysteretic Behavior of MFL, Second Floor.

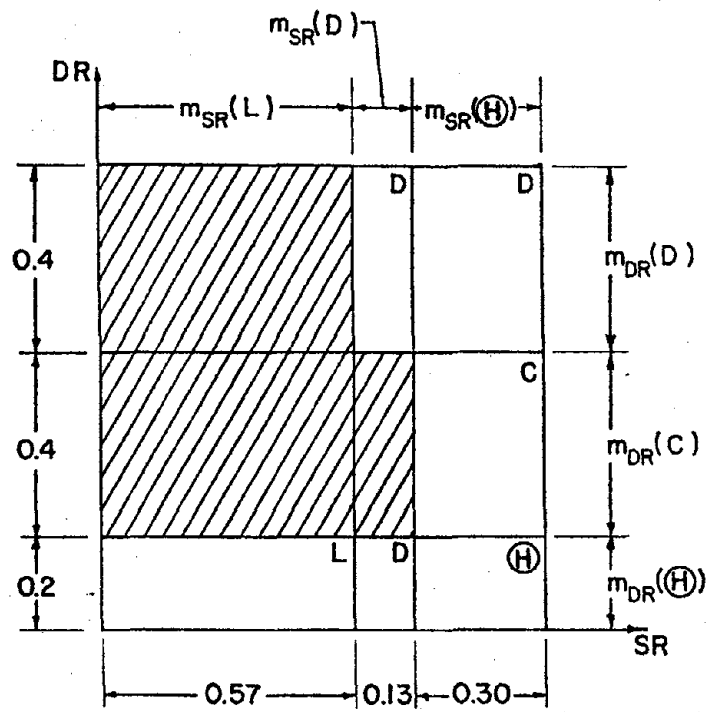


FIGURE 5

Dempster's Rule of Combination - Example

## STRUCTURAL ENGINEERING TECHNICAL REPORTS

- 81-3 "NFEAP - General Description, Sample Problems and User's Manual (1980 Version)", by S. S. Hsieh, E. C. Ting and W. F. Chen.
- 81-4 "Evaluation of Seismic Factor of Safety of a Submarine Slope by Limit Analysis", by C. J. Chang, W. F. Chen and J. T. P. Yao
- 81-5 "Inexact Inference for Rule-Based Damage Assessment of Existing Structures", by M. Ishizuka, K. S. Fu, and J. T. P. Yao. (PB80-235913)
- 81-6 "Theoretical Treatment of Certainty Factor in Production Systems", by M. Ishizuka, K. S. Fu, and J. T. P. Yao. (PB81-236457)
- 81-7 "Dynamic Stability of Curved Flow-Conveying Pipes", by E. C. Ting and Yi-Chen Liu.
- 81-8 "Cyclic Behavior of Tubular Sections", by S. Toma and W. F. Chen
- 81-9 "Structural Identification Control and Reliability in Wind Engineering Research", by J. T. P. Yao.
- 81-10 "Damage Assessment and Reliability of Existing Buildings", by J. T. P. Yao.
- 81-11 "Bibliography on Folded Plates (Theory, Material and Construction)" by C. D. Sutton and M. R. Resheidat
- 81-12 "NFEAP - General Description, Sample Problems and User's Manual (1980 Version) Part II", by S. S. Hsieh, E. C. Ting and W. F. Chen.
- 81-13 "Recent Advances on Analysis and Design of Steel Beam-Columns in USA", by W. F. Chen.
- 81-14 "Assessment of Seismic Displacements of a Submarine Slope by Limit Analysis", by C. J. Chang, W. F. Chen and J. T. P. Yao.
- 81-15 "Hystereses Identification of Multi-Story Buildings", by S. Toussi and J. T. P. Yao (PB81-235921)
- 81-16 "Inelastic Cyclic Analysis of Pin-Ended Tubes", by S. Toma and W. F. Chen.
- 81-17 "Cyclic Analysis of Fix-Ended Steel Beam-Columns", by S. Toma and W. F. Chen.
- 81-18 "Response of Truss Bridge to Traveling Vehicle", by E. C. Ting and J. Genin.
- 81-19 "Identification of Structural Characteristics Using Test Data and Inspection Results", by J. T. P. Yao
- 81-20 "Lateral Earth Pressures on Rigid Retaining Walls Subjected to Earthquake Forces", by M. F. Chang and W. F. Chen.
- 81-21 "Constitutive Relations and Failure Theories (Chapter 2)", by W. F. Chen (Chairman), Z. P. Bazant, O. Buyukozturk, T. Y. Chang, D. Darwin, T. C. Y. Liu and K. J. Willam.
- 81-22 "A Numerical Approach For Flow-Induced Vibration of Pipe Structures", by E. C. Ting and A. Hosseinipour.
- 81-23 "Seismic Safety Analysis of Submarine Slopes", by C. J. Chang, W. F. Chen and J. T. P. Yao.
- 81-24 "Inference Procedure with Uncertainty For Problem Reduction Method", by M. Ishizuka, K. S. Fu and J. T. P. Yao.
- 81-25 "Serviceability and Reliability of Antenna Structures in Part I: Theory", S. H. Wang, J. T. P. Yao and W. F. Chen.
- 81-26 "Fuzzy Statistics and Its Potential Applications in Civil Engineering", by J. T. P. Yao, K. S. Fu, M. Ishizuka.
- 81-27 "A Rule - Inference Method for Damage Assessment", by M. Ishizuka, K. S. Fu, and J. T. P. Yao.
- 81-28 "Lateral Load Capacity of Structural Tee X-Bracing", by A. D. M. Lewis and K. Nematollahi.
- 81-29 "Stability of Structural Members with Time Dependent Material Properties", by E. C. Ting and W. F. Chen
- 81-30 "Response of Plate Bridges to a Moving Mass", by J. Genin, E. C. Ting & Mehdi Ilkhani-Pour
- 81-31 "Probabilistic Methods for the Evaluation of Seismic Damage Of Existing Structures", by J. T. P. Yao
- 81-32 "Lok-Test - A Non-Destructive Concrete Compressive Test", by S. Mofid, W. F. Chen, M. J. Gutzwiller
- 81-33 "Cyclic Inelastic Behavior of Steel Tubular Beam-Columns", by D. J. Han and W. F. Chen
- 81-34 "Plasticity in Reinforced Concrete", by W. F. Chen
- 81-35 "Fatigue Reliability of Structures Under Combined Loading", by Wang Dian-Fu and J. T. P. Yao
- 81-36 "SPERIL I - Computer Based Structural Damage Assessment System", by M. Ishizuka, K. S. Fu and J. T. P. Yao
- 81-37 "Elastic-Plastic-Fracture Analysis of Concrete Structures", by H. Suzuki and W. F. Chen
- 81-38 "Strength of H-Columns with Small End Restraints", by E. M. Lui and W. F. Chen
- 82-1 "Cap Models for Clay Strata to Footing Loads," by E. Mizuno and W. F. Chen
- 82-2 "Plasticity Models for Seismic Analyses of Slopes," by E. Mizuno and W. F. Chen.
- 82-3 "Plastic Analysis of Slope with Different Flow Rules," by E. Mizuno and W. F. Chen.
- 82-4 "Large-Deformation Finite-Element Implementation of Soil Plasticity Models," by E. Mizuno and W. F. Chen
- 82-5 "Effects of Adjustable Gain and Delay Time of Control Systems to Structural Safety," by M.A. Basharkhah and J. T. P. Yao.
- 82-6 "Analysis of Steel Beam-to-Column Flange Connections," by K. V. Patel and W. F. Chen.
- 82-7 "Nonlinear Analysis of Steel Beam-to-Column Web Connections," by K. V. Patel and W. F. Chen.
- 82-8 "Accessories to NONSAP Program," by K. V. Patel and W. F. Chen.

